Domain-Generalizable Multiple-Domain Clustering

Anonymous authors
Paper under double-blind review

Abstract

This work generalizes the problem of unsupervised domain generalization to the case in which no labeled samples are available (completely unsupervised). We are given unlabeled samples from multiple source domains, and we aim to learn a shared predictor that assigns examples to semantically related clusters. Evaluation is done by predicting cluster assignments in previously unseen domains. Towards this goal, we propose a two-stage training framework: (1) self-supervised pre-training for extracting domain invariant semantic features. (2) multi-head cluster prediction with pseudo labels, which rely on both the feature space and cluster head prediction, further leveraging a novel prediction-based label smoothing scheme. We demonstrate empirically that our model is more accurate than baselines that require fine-tuning using samples from the target domain or some level of supervision.

1 Introduction

Accurately clustering high-dimensional measurements is vital for adequately analyzing scientific data. In recent years, deep learning-based frameworks have led to significant improvements compared to classical clustering models, such as K-means (Lloyd, 1982) or Spectral Clustering (Ng et al., 2001). However, if the observations are collected from multiple domains, classical and deep learning clustering models may group samples based on domain-specific information (such as style) rather than their semantic content. The problem becomes even more challenging if samples from the target domain are unavailable during training. Such a setting could occur due to privacy or computational considerations and has several applications, such as face clustering on edge devices Caldarola et al. (2021), medical images clustering Mittal et al. (2021), and more.

Towards this goal, we study the ability to learn a predictor f that, given a sample, regardless of its domain, can categorize it to its matching cluster. The requirement is that f is evaluated (one sample at a time) in an unseen target domain for which no sample is seen during training. This task combines the problem of multiple-domain clustering with domain generalization. Both of these are of high value, and their combination is extremely powerful: multiple source clustering is core to scientific discovery, e.g., in biomedicine, where a distribution shift exists between different individuals, and making accurate predictions on new domains is of the highest value Bae et al. (2022); Liu et al. (2022). While previous works consider a related problem, they all rely on partial supervision Zhang et al. (2021); Harary et al. (2022) or require access to target domain samples during training Gopalan (2017); Menapace et al. (2020).

Formally, the problem statement is as follows. We are given a dataset S with N samples from d domains, where each domain has $N_i, \forall i \in \{1, ..., d\}$ samples, and we know which sample belongs to each domain. A classifier f is trained to map every sample in S to one of K groups. A set of labeled examples is used for evaluation purposes only, and the K groups are assigned to a set of ground truth labels using a best-matching method (the Hungarian method Kuhn (1955)) on an unseen single-domain dataset T. Specifically, without further training, f is applied to each sample of T, and the predicted labels are compared to the ground truth labels of the samples in T.

We present a two-phase learning scheme for addressing the challenge of multiple-domain clustering with domain generalization. Our *pretraining stage* leverages a contrastive loss with several complementary components that encourage learning domain-agnostic representations. Specifically, we use style augmentations to reduce stylistic variations and an adversarial domain loss to eliminate the influence of domain-specific content. We further introduce a special queue procedure and domain balancing to stabilize the muti-domain training scheme. Next, we present several novel components to learn a multi-domain *clustering assigmnegts*. These include (i) a special pseudo-label selection procedure that exploits a style-augmented common domain to identify reliable labels. (ii) prediction-based label smoothing procedure that prevents mode collapse to highly populated clusters and bad initialization. (iii) a multiple clustering head prediction and filtration procedure to stabilize the clustering step in the presence of high-dimensional data or many categories.

We test our method on various multi-domain datasets and demonstrate its superiority over several strong baselines. Our framework is at par or better than state-of-the-art clustering methods but does not require any: (i) labeled data and (ii) adaptation to samples from the target domain. By removing these two requirements, our model opens the door to new applications in which labeled data is unavailable or access to target samples is infeasible due to privacy constraints. Additionally, our ablation studies validate the importance of each proposed component in contributing to the model's generalization capabilities.

2 Background and related work

Self-supervised learning (SSL) is a technique for extracting useful representation from unlabelled data using a pretext task. In computer vision, many methods rely on a contrastive loss; for example, SimCLR (Chen et al., 2020a) uses paired augmentations, creating feature representations that are projected and trained to maximize agreement. The seminal SSL framework MoCo (He et al., 2020) introduced a queue of negative samples and a momentum-moving average encoder to improve the contrastive learning framework.

Deep clustering aims to exploit the strength of neural networks (NN) as feature extractors to identify a representation that better preserves cluster structures using unlabelled data. DeepCluster (Caron et al., 2018) learns informative features and cluster assignments by iterating between applying k-means to the extracted features and training a NN to predict the cluster assignments. Ji et al. (2018) apply content-preserving image transformations to create pairs of samples with shared semantic information. Then, they train a NN to maximize the mutual information between the image pairs in a probabilistic data representation. Recently, Semantic Pseudo-Labeling for Image Clustering (Niu et al., 2022) obtained state-of-the-art results on several benchmarks. It is an iterative deep clustering method that relies on self-supervision and pseudo-labeling. First, self-

supervision is performed using a contrastive loss to learn informative features. Then, they create prototype pseudo labeling to avoid miss-annotations common to pseudo labeling techniques.

Unsupervised domain generalization (UDG) was recently presented by Zhang et al. (2021); Harary et al. (2022). UDG is related to our goal but requires some amount of supervision. Specifically, UDG involves: unsupervised training on a set of source domains, then fitting a classifier using a small number of labeled images. Finally, evaluating the model on a set of target domains unseen during training. Toward this goal, Zhang et al. (2021) suggests ignoring domain-related features by selecting negative samples from a queue based on their similarity to the positive sample domain. Recently, Harary et al. (2022) presented BrAD, in which self-supervised pre-training on multiple source domains is performed in a shared sketch-like domain. To fine-tune a classifier, they used various amounts of source domain-labeled samples. In contrast to these works, in our research, no class labels for either source or target domains are used for training the model. Furthermore, we do not assume knowledge about corresponding images between domains, only that all target classes appear in each domain.

Unsupervised Clustering under Domain Shift (UCDS) was presented by Menapace et al. (2020). The goal is to cluster samples from multiple source domains and then adapt the model to the target domain using multiple unlabeled samples from that domain. The authors suggest optimizing an information-theoretic loss coupled with domain-alignment layers. Figure 1 illustrates different approaches for multi-domain image classification. The UCDS setting is similar to ours; however, we aim to design a model that can predict cluster assignments on multiple source domains and generalize to new unseen domains without any further tuning or adaptation. To the best of our knowledge, this is the first work that solves this task without using any labels or samples from the target domain. This is a significant advantage since, in real-world settings, we often don't know that a domain shift occurred or can not access samples from the test domain due to privacy or computational considerations.

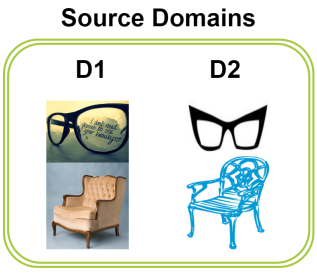

Training Data Required

Task	Source	Target
DA	LABELLED	LABELLED
UDA/DG	LABELLED	-
UDG	LIMITED	-
UCDS	UNLABELLED	UNLABELLED
Ours	UNLABELLED	-

Figure 1: Different tasks for multi-domain image classification: Domain adaptation (DA) requires both source and target domain labels at training time (Csurka et al., 2017). Unsupervised domain adaptation (UDA) and domain generalization (DG) remove the requirement for target domain labels (Roy et al., 2019; Matsuura & Harada, 2020). Unsupervised domain generalization (UDG) utilizes a limited amount of labels for the source domains and no labels for the target domain (Harary et al., 2022). Unsupervised clustering under domain shift (UCDS) does not use any labels but requires access to the unlabelled target domain for model fine-tuning (Menapace et al., 2020). Our approach does not require any labels or fine-tuning on the target domain.

3 Method

Our method consists of two phases; first, a feature extraction model f_e is trained in a self-supervised fashion on data from multiple source domains. This phase bridges the gap between different domains by extracting semantically related features $u_i \in \mathbb{R}^e$, where e is the embedding dimension. The second phase focuses on training a clustering head f_c while the weights of f_e are frozen. Then our cluster predictions are based on $f = f_c \circ f_e$.

The feature extraction step includes several pre-training stages designed for learning features that capture semantic information and attenuate the style content from each image. To train a domain invariant cluster predictor, we propose the following elements: data augmentation for clustering head training, reliable pseudo-label generation, clustering head training loss, prediction-based smoothing, and multiple clustering heads. A detailed description of these steps appears in the following subsections.

3.1 Pre-training

Our pre-training strategy generalizes MoCoV2 (Chen et al., 2020b) for multiple domains by introducing four components that enable learning robust domain-agnostic embeddings. First, we introduce style transfer augmentations, and using a contrastive loss, we learn a representation invariant to stylistic variations across domains. We further introduce an adversarial loss to eliminate domain-specific information at the distribution level. To stabilize the multi-domain contrastive training process, we introduce domain-specific queues, each tailored to a distinct domain. This prevents pushing apart representations from different domains and encourages learning content rather than domain-specific features. Additionally, we address domain imbalance by implementing a virtual balancing approach to mitigate the impact of population differences across domains. These pre-training components are detailed bellow, followed by a description of the contrastive learning framework used here.

1. *Style transfer augmentation:* We propose incorporating style augmentations into our contrastive loss to attenuate the influence of "style" on our extracted representation. Specifically, with probability p_{st} we perform a style transfer augmentation $\mathcal{ST}(x_i)$. This example is then fed into a contrastive loss with x_i that learns a mapping such that $\mathcal{ST}(x_i)$ and x_i are indistinguishable. To augment with varying styles of domains, we use Huang & Belongie (2017); this allows us to enhance the ability of our feature extractor to ignore domain-specific features.

2. *Adversarial loss:* We add a complementary step to remove domain-specific information at the distribution level. We achieve this using an adversarial domain loss Ganin & Lempitsky (2015). Specifically, we train our feature extractor f_e to learn features that are not influenced by domain identity. To do this, we "fool" a domain classifier f_d by updating the weights of f_e using a constant $\lambda_d \geq 0$ and the gradient of f_d denoted as $\frac{\partial \mathcal{L}_{f_d}}{\partial \theta_d}$. This technique is called a gradient reversal layer. This encourages the feature extractor to remove the domain-specific information. We note that the label of the domain is generally available for free; for instance, in medical applications, this could refer to the imaging technology.

3. *Domain-specific queues:* In contrastive training, negative samples are stored in queues. To avoid pushing apart the representations of different domains, we use multiple domain-specific queues Harary et al. (2022). Specifically, we introduce domain-specific queues $Q = [Q_1, Q_2, ..., Q_d]$ each

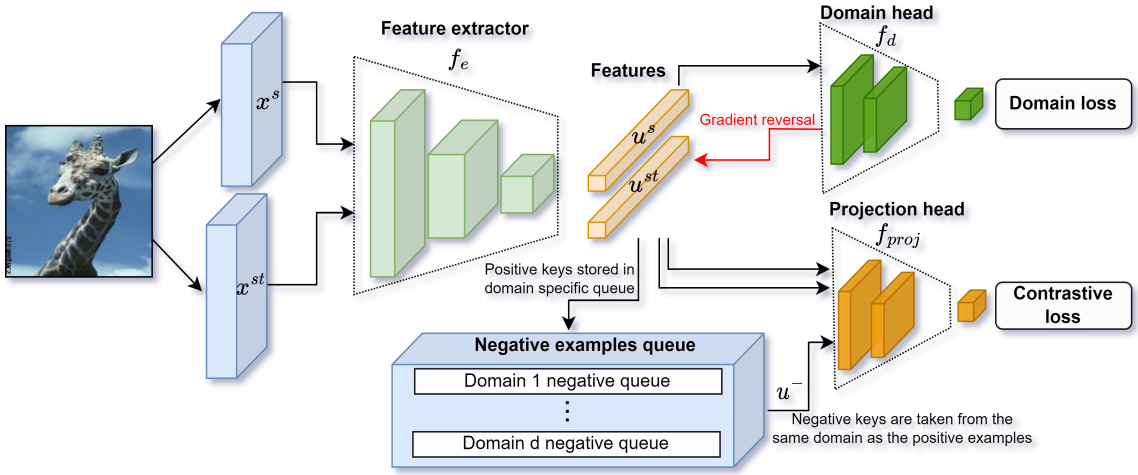

Figure 2: The proposed pre-training procedure. Each image is transformed using strong augmentations or style transfer augmentation. The features u^s (strong augmentation) and u^{st} (style augmentation) are extracted using f_e. Then we use a domain head f_d to classify the domain identity of each sample, minimizing the domain loss $\mathcal{L}_{f_d}$; we use gradient reversal to update the feature extractor f_e to fool the domain head in an adversarial fashion. The contrastive loss $\mathcal{L}_{f_{proj}}$ is minimized based on the output of the projection head u^s, u^{st}, and u^- (negative samples).

with size N_q for each of the d domains. The negative examples u_i^- are drawn from the same domain as the positive sample, which makes the discrimination more challenging and encourages the model to focus on the content rather than the domain. Positive samples u_i^+ are stored in the relevant domain queue for later use as negative examples.

4. *Domain balancing:*

The populations of samples from different domains may differ significantly. Such domain imbalance can cause poor generalization since the model might predominantly learn from the heavily populated domain. To address this issue, we employ a virtual balancing approach by sampling domain-balanced mini-batches. This strategy helps mitigate the domain imbalance, enhancing the model's ability to generalize more effectively across the different domains.

Pretraining overview We are given an input batch of images $x = [x_1, x_2, .., x_B]^T \in \mathbb{R}^{B\times C\times W\times H}$ where C, W, H represent color, width and height dimensions. Each image x_i is transformed twice. First, using a strong augmentation $x_i^s = \mathcal{S}(x_i)$. Second, the image is transformed using:

$$x_i^{st} = \begin{cases} \mathcal{ST}(x_i), & w.p \quad p_{st}, \\ \mathcal{S}(x_i) \quad , & w.p \quad 1 - p_{st}. \end{cases}$$

Where $\mathcal{ST}(x_i)$ replaces the style of x_i with another domain's style with probability p_{st}, otherwise, a strong augmentation $\mathcal{S}(x_i)$ is applied to generate the positive sample. Both x_i^s and x_i^{st} are passed through the feature extractor f_e to create the embeddings $u_i^s = \mathcal{P}(f_e(x_i^s, \theta_1), \theta_p)$, $u_i^{st} = \mathcal{P}(f_e(x_i^{st}, \theta_1^{'}), \theta_p^{'})$, where $\mathcal{P}$ and θ_p are the projection head and its weights respectively. $\theta_1^{'} = \mu\theta_1^{'} + (1-\mu)\theta_1$ and $\theta_p^{'} = \mu\theta_p^{'} + (1-\mu)\theta_p$ are the moving average versions of θ_1 and θ_p respectively. Finally, negative samples $u_i^-, \forall i \in [0, N_q]$ are sampled from a domain queue of the same domain d_{x_i}

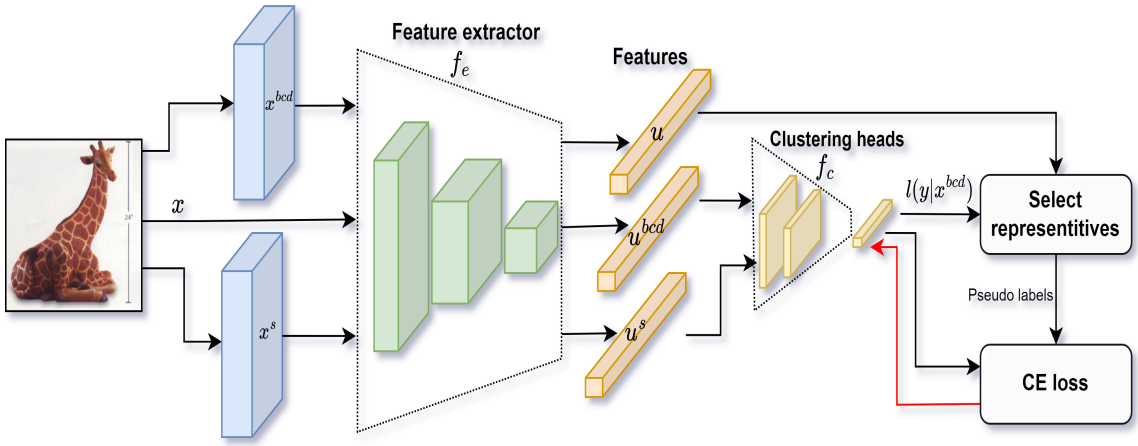

Figure 3: Clustering head training. The image is passed through the feature extractor f_e in its original (u), strongly augmented (u^s), and BCD form (u^{bcd}). The weights of f_e are frozen and used to produce the features. Representatives are selected from the original image features based on the clustering head's predictions over the BCD images. The class representatives are used as pseudo labels for the CE loss.

as x_i. We use the following contrastive loss:

$$\mathcal{L}_{f_{proj}} = -log \frac{exp((u^s)^T u^{st})}{\sum_{i=1}^{N_q} exp((u^s)^T u_i^-) + exp((u^s)^T u^{st})}, \tag{1}$$

where $u^s = [u_1^s, u_2^s, .., u_B^s]^T \in \mathbb{R}^{Bxe}$, $u^{st} = [u_1^{st}, u_2^{st}, .., u_B^{st}]^T \in \mathbb{R}^{Bxe}$, are the embeddings for the transformed input batch x^s, x^{st}.

To further remove domain-specific information, we use an additional domain adversarial term using a cross-entropy loss: $\mathcal{L}_{f_d} = -\mathcal{L}_{ce}(f_d(u^s), \theta_d)$. Hence, our complete objective is

$$\mathcal{L}_{f_e} = \mathcal{L}_{f_{proj}} + \mathcal{L}_{f_d}.$$

The contrastive loss term and domain-adversarial loss term help learn features that are related to the content and invariant to the domain.

3.2 Clustering predictor head

The pre-training phase provides a solid and robust feature extractor f_e on which a clustering head f_c can be trained. The clustering head should be able to separate multi-domain data into groups of samples with similar semantic content while ignoring the cross-domain distribution shifts. We do not assume that samples from the test domain are available during training, and we want to design a clustering head that can generalize to new unseen domains at inference time.

To obtain this goal, we present a clustering head training scheme for multi-domain assignments. First, we bridge domain gaps using a Basic Common Domain (BCD), transforming images into a sketch-like domain that retains object identity while reducing biases from color or style. The clustering head is then trained on strong augmentations and style-transferred images. Next, we generate reliable pseudo-labels based on the clustering head's predictions in the BCD (logits) $l(y|x^{bcd}) = f_c \circ f_e(x^{bcd})$, and the semantic features (embeddings) $u = f_e(x)$ of the original image.

We introduce multiple heads and select the most reliable ones by evaluating their *diversification* to enhance the clustering stability. Additionally, we present a new prediction-based label smoothing, adjusting label uncertainties based on past prediction statistics and promoting robust learning across domains. This holistic strategy ensures effective clustering in high-dimensional image data while addressing the challenges of domain gaps and instability inherent in the clustering process. These steps are detailed below, and the training procedure is illustrated in Figure 3.

1. *Data augmentation for clustering head training:* We leverage a BCD to mitigate the gap between several domains. The BCD is designed to maintain the content of each sample while removing domain-related information. A sketch-like domain can be considered a suitable BCD for image data with varying color and texture domains. Transforming an image to a sketch domain keeps high-level features such as object identity while decreasing the bias induced by color or style-preserving features. The clustering head is trained by sampling a batch of B images from all source domains. Each sample x_i passes through f_e in three different versions. Based on the original image, and using two transformations: a strong augmentation $x_i^s = \mathcal{E}(x_i)$, and style transfer to our BCD $x_i^{bcd} = \mathcal{C}(x_i)$. Where $\mathcal{C}()$ represents a style transfer (see the Pre-training section) of the input image x_i to an image with a sketch-like style Huang & Belongie (2017). $\mathcal{E}()$ is defined as:

$$x_i^{st} = \begin{cases} \mathcal{C}(x_i) & , \quad w.p \quad p_{st}p_{bcd} \\ \mathcal{ST}(x_i), & w.p \quad p_{st}(1-p_{bcd}), \\ \mathcal{S}(x_i) & , \quad w.p \quad 1-p_{st}. \end{cases}$$

The BCD transformed and the original images are used to define the pseudo labels, while the strong augmentations are used to train the clustering head f_c, as detailed below.

2. *Reliable pseudo label generation:* First, features are extracted from the original image: $u = f_e(x, \theta_1)$. Then, logits are extracted in the BCD based on: $l(y|x^{bcd}) = f(x^{bcd}) = f_c \circ f_e(x^{bcd})$. The top $\gamma := \frac{B}{2K}$ samples are chosen from $l(y|x_i^{bcd})$ as the set of most confident samples of class k based on the clustering head's score on samples from the BCD. Thus, the selected samples are denoted as follows:

$$\mathcal{M}_k = \{u_i | i \in argtop\gamma(l(k|x^{bcd})), \forall i \in \{1, ..., B\}\}, \tag{2}$$

where $argtop\gamma(l(k|x^{bcd})) \in \mathbb{N}^\gamma$ is a vector of indexes that chooses the γ most confident samples, based on their corresponding BCD score $l(k|x^{bcd})$. $\mathcal{M}_k$ is a set of γ embedding vectors. Using M_k, the center of class k is determined by:

$$G_k = \frac{1}{\gamma} \sum_{u_i \in \mathcal{M}_k} u_i. \tag{3}$$

One can calculate the similarity between each sample and each of the centers: $sim_k = \langle \bar{G}_k, \bar{u} \rangle$. Where $\bar{G}_k = \frac{G_k}{\|G_k\|}$, and $\bar{u} = \frac{u}{\|u\|}$ are the normalized feature and center vectors, respectively. Specifically, $sim_k \in \mathbb{R}^B$ represents how close each sample in the batch is to the center of cluster k.

Samples that are closest to the center are used as pseudo labels for cluster k; thus, the set of strongly augmented data samples with pseudo labels is formulated as follows:

$$\hat{\mathcal{Z}}_k = \{x^s[argtop\gamma(sim_k)], k\}. \tag{4}$$

Where $x^s[argtop\gamma(sim_k)]$ means indexing x^s using $argtop\gamma(sim_k)$, i.e., choosing the samples that will be used as pseudo-labels for class k using the similarity in the embedding domain. While M_k

are chosen based on the predictions in the logit space, $\hat{\mathcal{Z}}_k$ are pseudo labels based on information from both the semantic space Eqs. 3,4 and in the logits space Eq. 2. Using only the logit values to infer the pseudo labels results in poor cluster assignments, as demonstrated in our ablation study. The entire set of representatives and pseudo-label pairs will be denoted as $\hat{\mathcal{Z}}$.

3. *Clustering head training loss:* In the second phase, the clustering head f_c is trained using $\hat{\mathcal{Z}}$ to minimize cross-entropy loss using the pseudo labels. A batch of samples and pseudo labels $(x^s_{pl}, y_{pl}) \in \hat{\mathcal{Z}}$, are propagated through f_c, and f_e, and the objective can be formulated as:

$$\mathcal{L} = \frac{1}{B}\mathcal{L}_{ce}(f_c \circ f_e(x_{pl}), y_{pl}). \tag{5}$$

During this training phase, domain balancing is used, as detailed in our pre-training section.

4. *Prediction-based label smoothing:* Label smoothing Szegedy et al. (2016) prevents a classifier from being overconfident, which may lead the classifier to collapse to specific classes and neglect the rest. Using past prediction statistics, we present an improved label smoothing that varies the smoothing intensity between clusters. We perform stronger smoothing for frequently predicted clusters and vice versa. Specifically, let $\hat{y}(x) \in \{0,1\}^K$ be the one-hot prediction of sample x, and we denote the empirical density of predictions over the batch as $\mathcal{H}_{cur} \in \mathbb{R}^K$. We further compute the exponential moving average of prediction density as $\mathcal{H} = \alpha * \mathcal{H} + (1-\alpha)\mathcal{H}_{cur}$ with $\alpha \in (0,1)$ is a constant for balancing between history and current statistics. We perform our cluster-specific prediction-based label smoothing using $\mathcal{H}$. Precisely, for cluster $k \in K$ we define the smoothed pseudo-label as $\bar{y}_{pl}[k] = \max(1 - \mathcal{H}[k], s_{min})$, where s_{min} is the minimal smoothing value, and the values of the remaining clusters are spread uniformly to sum up to 1.

5. *Multiple clustering heads:* Clustering is inherently unstable, especially when dealing with many classes or high-dimensional datasets. Several authors have proposed using feature selection (Solorio-Fernández et al., 2020; Shaham et al., 2022; Lindenbaum et al., 2021) to improve clustering capabilities by removing nuisance features in tabular data. We are interested in stabilizing clustering performance on diverse high-dimensional image data. Therefore, we propose training multiple clustering heads simultaneously and selecting a reliable head based on an unsupervised criterion. This allows us to handle many categories and overcome the instability that stems from random weight initialization. For more details about the source of randomization between heads, please see Appendix B.3. The number of clustering heads is denoted as h, hence the objective in Eq. 5, $\mathcal{L}$ can now be formulated as the average of the h head specific losses:

$$\mathcal{L} = \frac{1}{Bh}\sum_{i=1}^{h}\mathcal{L}^i_{ce}(f_c \circ f_e(x_{pl}), y_{pl_s}). \tag{6}$$

Next, we define the *diversification* of head j as:

$$dv_j = |\{argmax_{k\in K} l_j(y|x)/K\}|. \tag{7}$$

First, $argmax$ reduces the prediction $l_j(y|x)$ of the j-th head to a cluster index. Next, we use the operator $|.|$, which counts the number of distinct cluster predictions in the set of predictions by head j; this process is performed over the entire dataset without any parameter update.

Due to high variability in the training procedure between heads, some are better than others; we leverage this variability by keeping only the most diversified heads (MDH). Two MDH are chosen

out of h clustering heads based on higher dv_j values compared to the other heads. The heads with lower dv_j are discarded, and we replace the weights of the non-MDH with a linear combination of the two MDH weights. Mathematically speaking, let us define θ_{2_i} as the weights of the i-th head, and let us assume that j, k are the MDH indices; hence the weights of the non-MDH heads are overridden in the following manner:

$$\theta_{2_i} = r_k \theta_{2_k} + r_j \theta_{2_j}, \forall i \neq k, j. \tag{8}$$

Where $r_k \sim \mathcal{U}(0, 1)$ and $r_j = 1 - r_k$. Inspired by recent weight averaging works (Jain et al., 2023; Yin et al., 2023; Wortsman et al., 2022), this removes the influence of non-diverse heads and maintains some degree of variability for the following optimization steps.

In cases where there is equality in dv_j between several heads, which results in more than two MDHs, we limit the number of MDHs to five. The rationale behind this limitation can be elucidated through the following illustrative scenario, w.l.o.g., assume that the first head does not predict one class, and the other heads do not predict five classes; if the number of MDH kept is not limited, the advantage of the first head is not utilized. Since all heads will perform poorly in the early training phase, MDH selection is initiated after a few epochs. Furthermore, to allow the heads to make gradual learning, the process repeats every n epochs.

4 Experiments

Experiments are conducted using four datasets commonly used to evaluate domain generalization methods. Representative images from several datasets and domains appear in Appendix C. **Office31** dataset (Saenko et al., 2010) consists of images collected from three domains: Amazon, Webcam, and DSLR, with 2817, 795, and 498 images, respectively. The dataset includes 31 different classes shared across all domains. The samples consist of objects commonly encountered in an office setting. **PACS** dataset (Li et al., 2017) consists of four domains: Sketch, Cartoon, Photo, and Artpainting with 3929, 2344, 1670, and 2048 images, respectively. It includes seven different classes, which are shared across all domains. **Officehome** dataset (Venkateswara et al., 2017) contains four domains: Art, Product, Realworld, and Clipart, with 2427, 4439, 4357, and 4365 images, respectively. It includes 65 different classes, which are shared across all domains. The large number of domains and classes makes the task challenging. In particular, since we aim to cluster the data without access to labeled observations. Existing state-of-the-art results on this data (Menapace et al., 2020) corroborate this claim. **DomainNet** dataset, introduced by Peng et al. (2019), consists of six domains: Real, Painting, Sketch, Clipart, Infograph, and Quickdraw. It includes about 0.6 million images (48K - 172K per domain) distributed among 345 classes.

Baselines To evaluate the capabilities of our model, we focus on the following scheme: train the model using d unlabelled source domains, then evaluate our model on the unseen and unlabelled target domain. We compare our approach to several recently proposed deep learning-based clustering models for multi-domain data. Our implementation details appear in Appendix B.1.

When evaluating Office31 and Officehome datasets, we compare with ACIDS (Menapace et al., 2020), Invariant Information Clustering for Unsupervised Image Classification and Segmentation (IIC) (Ji et al., 2018), and DeepCluster (Caron et al., 2018). Importantly, they were trained directly on the target domain before predicting the clusters. We further compare two variations of IIC, specifically, IIC-Merge involves training IIC on all domains, including the target domain;

Method	Target fine-tuned	Supervision	$D, W \to A$	$A, W \to D$	$A, D \to W$	Avg
DeepCluster (Caron et al., 2018)	✓	-	19.6	18.7	18.9	19.1
IIC (Ji et al., 2018)	✓	-	31.9	34.0	37.0	34.3
IIC-Merge (Ji et al., 2018)	✓	-	29.1	36.1	33.5	32.9
IIC + DIAL (Ji et al., 2018)	✓	-	28.1	35.3	30.9	31.4
Continuous DA (Mancini et al., 2019)	✓	-	20.5	28.8	30.6	26.6
ACIDS (Menapace et al., 2020)	✓	-	**33.4**	36.1	37.5	35.6
K-means (Lloyd, 1982)	✓	-	14.9	24.3	20.8	29.9
Ours	-	-	24.1	**50.1**	**47.7**	**40.6**

Table 1: Accuracy results on the Office31 dataset (31 classes) upon all three domain combinations, each of the letters A, W, D represent the domains Amazon, Webcam, and DSLR, respectively. The notation $X, Y \to Z$, means the model was trained on X, Y domain and tested on the Z domain. Target fine-tuned means the method was trained or adapted to the test domain. In K-means, we first pre-trained the MocoV2 model and trained K-means on top of its embeddings.

Method	Target fine-tuned	Supervision	$C, P, R \to A$	$A, P, R \to C$	$A, C, R \to P$	$A, C, P \to R$	Avg
DeepCluster (Caron et al., 2018)	✓	-	8.9	11.1	16.9	13.3	12.6
IIC (Ji et al., 2018)	✓	-	12.0	15.2	22.5	15.9	16.4
IIC-Merge(Ji et al., 2018)	✓	-	11.3	13.1	16.2	12.4	13.3
IIC + DIAL(Ji et al., 2018)	✓	-	10.9	12.9	15.4	12.8	13.0
Continuous DA (Mancini et al., 2019)	✓	-	10.2	11.5	13.0	11.7	11.6
ACIDS (Menapace et al., 2020)	✓	-	12.0	16.2	23.9	15.7	17.0
K-means (Lloyd, 1982)	✓	-	9.1	11.3	13.8	10.6	11.2
Ours	-	-	**20.8**	**26.2**	**27.7**	**27.2**	**25.5**

Table 2: Results on Officehome dataset (65 classes) upon all four domain combinations, each of the letters A, P, R, C represent the domains Art, Product, Realworld, and Clipart, respectively. The notation $W, X, Y \to Z$, means the model was trained on W, X, Y domain and tested on the Z domain. Target fine-tuned means the method was trained or adapted to the test domain. In K-means, we pre-train the MocoV2 model and then train K-means on top of its embeddings.

IIC+DIAL: IIC, which contains a domain-specific batch norm layer jointly trained on all domains. We further compare to continuous domain adaptation (Continuous DA) (Mancini et al., 2019), which trains on d domains, then adapted and tested on the target domain. Note that all the former baselines compared with our work were trained on the target domain. We added another baseline, training MoCoV2 on all the source domains and fitting the K-means clustering algorithm on the target domain.

On the PACS dataset, we also compared to BrAD (Harary et al., 2022) with various amounts of source domain labels. This comparison is very challenging as we do not use any class labels. Evaluation on DomainNet (Peng et al., 2019) was done following the protocol for UDG introduced in Zhang et al. (2021). Our method does not utilize labels compared to other methods, which use 1% source domain labels.

Results Table 1 depicts the results on all three domain combinations of Office31 dataset. On both DSLR and Webcam as target domains, our method outperforms the current state-of-the-art (SOTA) by a large margin, even without adaptation to the target domain. Our method performance on the Amazon domain is inferior to the current SOTA, which limited source domain data may explain. The target fine-tuned method (unsupervised fine-tuning on the target domain) relies on 317% more data for their training scheme. On average, our method is better by 10.1% than methods that use the target domain for adaptation and 31.1% over baselines with the same conditions.

Results on the Officehome dataset can be seen in Table 2. This dataset is more challenging than the former and consists of four domains. Our method outperforms the baselines on all four domain combinations and is better on average by 47.1% than the previous SOTA.

On the PACS dataset (Table 3), we compare to target fine-tuned and limited source domain label methods. Our method outperforms the current SOTA on 3 out of 4 target domains for the target fine-tuned case. Our method achieves slightly lower results on the fourth domain (Sketch) than the current target fine-tuned SOTA. This can be explained by a large amount of additional Sketch domain data (65%), exploited by baselines fine-tuned on the target domain. On average, our method outperforms all baselines that do not require any level of supervision. When comparing the two variations of BrAD with 1% source domain labels, we achieve superior results on all domains. Overall, our method outperforms BrAD-KNN, even though BrAD-KNN uses 10% of the source domain labels.

Table 4 illustrates the results on DomainNet dataset (Peng et al., 2019). Our method is compared to different SOTA UDG methods that use 1% of source domain labels. Although our method does not use any class labels, it outperforms all previous schemes across all domains by a large margin.

Ablation study We performed two ablation studies; the first examines different variants of our model, and the second focuses on the proposed prediction-based smoothing. In the first ablation

Method	Target fine-tuned	Supervision	$C,P,S \to A$	$A,P,S \to C$	$A,C,S \to P$	$A,C,P \to S$	Avg
DeepCluster(Caron et al., 2018)	✓	-	22.2	24.4	27.9	27.1	25.4
IIC (Ji et al., 2018)	✓	-	39.8	39.6	70.6	46.6	49.1
IIC-Merge (Ji et al., 2018)	✓	-	32.2	33.2	56.4	30.4	38.1
IIC + DIAL(Ji et al., 2018)	✓	-	30.2	30.5	50.7	30.7	35.3
Continuous DA (Mancini et al., 2019)	✓	-	35.2	34.0	44.2	42.9	39.1
ACIDS (Menapace et al., 2020)	✓	-	42.1	44.5	64.4	**51.1**	50.5
K-means (Lloyd, 1982)	✓	-	17.7	18.5	21.1	22.4	19.9
Ours	-	-	**47.3**	**45.4**	**66.6**	48.0	**51.8**
BrAD (Harary et al., 2022)	-	1%	33.6	43.5	61.8	36.4	43.8
BrAD-KNN (Harary et al., 2022)	-	1%	35.5	38.1	55.0	34.1	40.7
BrAD (Harary et al., 2022)	-	5%	41.4	50.9	65.2	50.7	52.0
BrAD-KNN (Harary et al., 2022)	-	5%	39.1	45.4	58.7	46.1	47.3
BrAD (Harary et al., 2022)	-	10%	44.2	50.0	72.2	55.7	55.5
BrAD-KNN (Harary et al., 2022)	-	10%	42.0	45.3	67.2	50.0	51.1

Table 3: Results on PACS dataset (7 classes) upon all four domain combinations, each letter A, P, S, C represents the domains: Art painting, Photo, Sketch, and Cartoon, respectively. The notation $W, X, Y \to Z$, means the model was trained on W, X, Y domain and tested on the Z domain. Target fine-tuned means the method was trained or adapted to the test domain. In K-means, we first pre-trained the MocoV2 model and trained K-means on top of its embeddings.

Method	Supervision	clipart, infograph, quickdraw			painting, real, sketch			Avg
		→ painting	→ real	→ sketch	→ clipart	→ infograph	→ quickdraw	
DIUL (Zhang et al., 2021)	1%	14.5	21.7	21.3	18.5	10.6	12.7	16.6
DiMEA (Yang et al., 2022)	1%	20.2	30.8	20.0	26.5	15.5	15.5	21.4
BrAD-KNN (Harary et al., 2022)	1%	16.9	22.3	25.7	40.7	14.0	21.3	23.5
BrAD (Harary et al., 2022)	1%	20.0	25.1	31.7	47.3	16.9	23.7	27.5
Ours	-	**27.0**	**29.0**	**40.0**	**52.2**	**17.4**	**32.4**	**33.0**

Table 4: Accuracy results on DomainNet dataset (Peng et al., 2019) upon two source domain combinations. The notation $X, Y \to Z$, means the model was trained on X, Y domain and tested on the Z domain. Without using any labels, our results outperform other SOTA UDG methods, which use 1% of source domain labels.

Method	C, P, S $\rightarrow A$	A, P, S $\rightarrow C$	A, C, S $\rightarrow P$	A, C, P $\rightarrow S$	Avg
Logits only	NA	NA	NA	NA	NA
Plain pre-training	25.0	22.7	29.8	NA	NA
No style transfer	40.6	37.2	50.2	45.8	43.5
No domain head	40.2	41.5	58.6	42.8	45.8
No smoothing	48.2	44.5	56.8	46.6	49.0
Label smoothing	46.3	44.4	**66.6**	**49.0**	51.6
Pred. based smoothing	**47.3**	**45.4**	**66.6**	48.0	**51.8**

Table 5: Ablation study on the PACS dataset. The letters A, P, S, C represent the domains Art painting, Photo, Sketch, and Cartoon, respectively. The arrow notation is similar to other tables. We denote by NA cases in which some of the classes were not predicted by the model, which makes calculating clustering accuracy unavailable.

study, we use the PACS dataset. The first variant of our model, which we term "Plain pre-training", uses a standard MoCoV2 feature extractor followed by training the clustering heads. In the second ablation, we omit the style transfer augmentation in pre-training and clustering head training. A third ablation, "no domain head," is performed using the full training procedure except for the domain head and its adversarial loss. The fourth ablation on the PACS dataset was done by removing the label smoothing (using 1 as the smoothing value). As the results presented in Table 5 indicate, our model performs better than all its ablated versions. This suggests that all proposed components contribute to our ability to generalize to unseen domains. In cases where not all clusters were predicted, and thus, no clustering accuracy can be calculated (NA). In the second ablation study, we focus on variations of label smoothing: no smoothing, standard label smoothing (Szegedy et al., 2016), and prediction-based smoothing. Our evaluation is conducted on PACS, Officehome, and Office31 datasets. Our results demonstrate that the proposed prediction-based smoothing improves clustering capabilities across all evaluated datasets. We provide results on PACS in Table 5, and results on the remaining datasets appear in Appendix B.4. We have omitted the results indicating the "single head" ablated version of our model since its prediction often did not cover all clusters.

Hyperparameter stability We use PACS and Officehome datasets to evaluate our model's sensitivity to hyperparameters. We test three hyperparameters and present our results in Appendix B.5 suggesting that our method is nearly insensitive to slight variations in the hyperparameters.

5 Discussion

Conclusion: We introduce a fully unsupervised multi-source domain generalized clustering framework. To the best of our knowledge, this paper presents, for the first time, a framework where no class labels are used for either source or target domains. Additionally, our solution does not require any adaptation to the target domain, resulting in better generalization abilities to previously unseen domains. Our approach outperforms all existing baselines and is evaluated in a more stringent and realistic setting. We consider several future directions: extending our model to other modalities, such as audio and text, and generalizing the clustering task to other important unsupervised learning tasks, such as anomaly detection or feature selection. We also plan to provide a theoretical analysis of our results. We believe our idea has great potential to advance the unsupervised multi-domain regime and be applied in other future research.

Limitations One limitation of our method is handling datasets with an extreme number of classes. One possible way to mitigate this issue is to use weak supervision. Furthermore, our current implementation can not accommodate non-overlapping classes between the training and testing subsets. Handling this issue is an interesting question for future research.

References

Sungwoo Bae, Kwon Joong Na, Jaemoon Koh, Dong Soo Lee, Hongyoon Choi, and Young Tae Kim. Celldart: cell type inference by domain adaptation of single-cell and spatial transcriptomic data. *Nucleic acids research*, 50(10):e57–e57, 2022.

Debora Caldarola, Massimiliano Mancini, Fabio Galasso, Marco Ciccone, Emanuele Rodolà, and Barbara Caputo. Cluster-driven graph federated learning over multiple domains. In *Proceedings of the IEEE/CVF Conference on Computer Vision and Pattern Recognition*, pp. 2749–2758, 2021.

Mathilde Caron, Piotr Bojanowski, Armand Joulin, and Matthijs Douze. Deep clustering for unsupervised learning of visual features. In *Proceedings of the European conference on computer vision (ECCV)*, pp. 132–149, 2018.

Ting Chen, Simon Kornblith, Mohammad Norouzi, and Geoffrey Hinton. A simple framework for contrastive learning of visual representations. In *International conference on machine learning*, pp. 1597–1607. PMLR, 2020a.

Xinlei Chen, Haoqi Fan, Ross Girshick, and Kaiming He. Improved baselines with momentum contrastive learning. *arXiv preprint arXiv:2003.04297*, 2020b.

Gabriela Csurka et al. *Domain adaptation in computer vision applications*, volume 2. Springer, 2017.

Ekin D Cubuk, Barret Zoph, Jonathon Shlens, and Quoc V Le. Randaugment: Practical automated data augmentation with a reduced search space. In *Proceedings of the IEEE/CVF conference on computer vision and pattern recognition workshops*, pp. 702–703, 2020.

Terrance DeVries and Graham W. Taylor. Improved regularization of convolutional neural networks with cutout, 2017. URL `https://arxiv.org/abs/1708.04552`.

Yaroslav Ganin and Victor Lempitsky. Unsupervised domain adaptation by backpropagation. In *International conference on machine learning*, pp. 1180–1189. PMLR, 2015.

Raghuraman Gopalan. Image clustering under domain shift. In *2017 IEEE Third International Conference on Multimedia Big Data (BigMM)*, pp. 74–77. IEEE, 2017.

Sivan Harary, Eli Schwartz, Assaf Arbelle, Peter Staar, Shady Abu-Hussein, Elad Amrani, Roei Herzig, Amit Alfassy, Raja Giryes, Hilde Kuehne, et al. Unsupervised domain generalization by learning a bridge across domains. In *Proceedings of the IEEE/CVF Conference on Computer Vision and Pattern Recognition*, pp. 5280–5290, 2022.

Kaiming He, Xiangyu Zhang, Shaoqing Ren, and Jian Sun. Deep residual learning for image recognition. In *Proceedings of the IEEE conference on computer vision and pattern recognition*, pp. 770–778, 2016.

Kaiming He, Haoqi Fan, Yuxin Wu, Saining Xie, and Ross Girshick. Momentum contrast for unsupervised visual representation learning. In *Proceedings of the IEEE/CVF conference on computer vision and pattern recognition*, pp. 9729–9738, 2020.

Xun Huang and Serge Belongie. Arbitrary style transfer in real-time with adaptive instance normalization. In *Proceedings of the IEEE international conference on computer vision*, pp. 1501–1510, 2017.

Samyak Jain, Sravanti Addepalli, Pawan Kumar Sahu, Priyam Dey, and R Venkatesh Babu. Dart: Diversify-aggregate-repeat training improves generalization of neural networks. In *Proceedings of the IEEE/CVF Conference on Computer Vision and Pattern Recognition*, pp. 16048–16059, 2023.

Xu Ji, Joao F Henriques, and Andrea Vedaldi. Invariant information distillation for unsupervised image segmentation and clustering. *arXiv preprint arXiv:1807.06653*, 2(3):8, 2018.

Harold W. Kuhn. The Hungarian Method for the Assignment Problem. *Naval Research Logistics Quarterly*, 2(1–2):83–97, March 1955. doi: 10.1002/nav.3800020109.

Da Li, Yongxin Yang, Yi-Zhe Song, and Timothy M Hospedales. Deeper, broader and artier domain generalization. In *Proceedings of the IEEE international conference on computer vision*, pp. 5542–5550, 2017.

Ofir Lindenbaum, Uri Shaham, Erez Peterfreund, Jonathan Svirsky, Nicolas Casey, and Yuval Kluger. Differentiable unsupervised feature selection based on a gated laplacian. *Advances in Neural Information Processing Systems*, 34:1530–1542, 2021.

Yan Liu, He Yan, Long-Chen Shen, and Dong-Jun Yu. Learning cell annotation under multiple reference datasets by multisource domain adaptation. *Journal of Chemical Information and Modeling*, 63(1):397–405, 2022.

Stuart P. Lloyd. Least squares quantization in pcm. *IEEE Trans. Inf. Theory*, 28(2):129–136, 1982. URL `http://dblp.uni-trier.de/db/journals/tit/tit28.html#Lloyd82`.

Massimiliano Mancini, Samuel Rota Bulo, Barbara Caputo, and Elisa Ricci. Adagraph: Unifying predictive and continuous domain adaptation through graphs. In *Proceedings of the IEEE/CVF Conference on Computer Vision and Pattern Recognition*, pp. 6568–6577, 2019.

Toshihiko Matsuura and Tatsuya Harada. Domain generalization using a mixture of multiple latent domains. In *Proceedings of the AAAI Conference on Artificial Intelligence*, volume 34, pp. 11749–11756, 2020.

Willi Menapace, Stéphane Lathuilière, and Elisa Ricci. Learning to cluster under domain shift. In *European Conference on Computer Vision*, pp. 736–752. Springer, 2020.

Himanshu Mittal, Avinash Chandra Pandey, Raju Pal, and Ashish Tripathi. A new clustering method for the diagnosis of covid19 using medical images. *Applied Intelligence*, 51:2988–3011, 2021.

Andrew Ng, Michael Jordan, and Yair Weiss. On spectral clustering: Analysis and an algorithm. In T. Dietterich, S. Becker, and Z. Ghahramani (eds.), *Advances in Neural Information Processing Systems*, volume 14. MIT Press, 2001. URL `https://proceedings.neurips.cc/paper/2001/file/801272ee79cfde7fa5960571fee36b9b-Paper.pdf`.

Chuang Niu, Hongming Shan, and Ge Wang. SPICE: Semantic pseudo-labeling for image clustering. *IEEE Transactions on Image Processing*, 31:7264–7278, 2022. doi: 10.1109/tip.2022.3221290. URL https://doi.org/10.1109%2Ftip.2022.3221290.

Adam Paszke, Sam Gross, Francisco Massa, Adam Lerer, James Bradbury, Gregory Chanan, Trevor Killeen, Zeming Lin, Natalia Gimelshein, Luca Antiga, Alban Desmaison, Andreas Kopf, Edward Yang, Zachary DeVito, Martin Raison, Alykhan Tejani, Sasank Chilamkurthy, Benoit Steiner, Lu Fang, Junjie Bai, and Soumith Chintala. Pytorch: An imperative style, high-performance deep learning library. In *Advances in Neural Information Processing Systems 32*, pp. 8024–8035. 2019.

Xingchao Peng, Qinxun Bai, Xide Xia, Zijun Huang, Kate Saenko, and Bo Wang. Moment matching for multi-source domain adaptation. In *Proceedings of the IEEE/CVF international conference on computer vision*, pp. 1406–1415, 2019.

Subhankar Roy, Aliaksandr Siarohin, Enver Sangineto, Samuel Rota Bulo, Nicu Sebe, and Elisa Ricci. Unsupervised domain adaptation using feature-whitening and consensus loss. In *Proceedings of the IEEE/CVF Conference on Computer Vision and Pattern Recognition*, pp. 9471–9480, 2019.

Kate Saenko, Brian Kulis, Mario Fritz, and Trevor Darrell. Adapting visual category models to new domains. In *European Conference on Computer Vision*, 2010.

Uri Shaham, Ofir Lindenbaum, Jonathan Svirsky, and Yuval Kluger. Deep unsupervised feature selection by discarding nuisance and correlated features. *Neural Networks*, 152:34–43, 2022.

Saúl Solorio-Fernández, J Ariel Carrasco-Ochoa, and José Fco Martínez-Trinidad. A review of unsupervised feature selection methods. *Artificial Intelligence Review*, 53(2):907–948, 2020.

Christian Szegedy, Vincent Vanhoucke, Sergey Ioffe, Jon Shlens, and Zbigniew Wojna. Rethinking the inception architecture for computer vision. In *Proceedings of the IEEE conference on computer vision and pattern recognition*, pp. 2818–2826, 2016.

Wouter Van Gansbeke, Simon Vandenhende, Stamatios Georgoulis, Marc Proesmans, and Luc Van Gool. Scan: Learning to classify images without labels. In *European conference on computer vision*, pp. 268–285. Springer, 2020.

Hemanth Venkateswara, Jose Eusebio, Shayok Chakraborty, and Sethuraman Panchanathan. Deep hashing network for unsupervised domain adaptation. In *Proceedings of the IEEE Conference on Computer Vision and Pattern Recognition*, pp. 5018–5027, 2017.

Rui Wang, Zuxuan Wu, Zejia Weng, Jingjing Chen, Guo-Jun Qi, and Yu-Gang Jiang. Cross-domain contrastive learning for unsupervised domain adaptation. *IEEE Transactions on Multimedia*, 2022.

Mitchell Wortsman, Gabriel Ilharco, Samir Ya Gadre, Rebecca Roelofs, Raphael Gontijo-Lopes, Ari S Morcos, Hongseok Namkoong, Ali Farhadi, Yair Carmon, Simon Kornblith, et al. Model soups: averaging weights of multiple fine-tuned models improves accuracy without increasing inference time. In *International Conference on Machine Learning*, pp. 23965–23998. PMLR, 2022.

Haiyang Yang, Shixiang Tang, Meilin Chen, Yizhou Wang, Feng Zhu, Lei Bai, Rui Zhao, and Wanli Ouyang. Domain invariant masked autoencoders for self-supervised learning from multi-domains. In *Computer Vision–ECCV 2022: 17th European Conference, Tel Aviv, Israel, October 23–27, 2022, Proceedings, Part XXXI*, pp. 151–168. Springer, 2022.

Lu Yin, Shiwei Liu, Meng Fang, Tianjin Huang, Vlado Menkovski, and Mykola Pechenizkiy. Lottery pools: Winning more by interpolating tickets without increasing training or inference cost. In *Proceedings of the AAAI Conference on Artificial Intelligence*, volume 37, pp. 10945–10953, 2023.

Xingxuan Zhang, Linjun Zhou, Renzhe Xu, Peng Cui, Zheyan Shen, and Haoxin Liu. Towards Unsupervised Domain Generalization. *arXiv e-prints*, art. arXiv:2107.06219, July 2021.

Xingxuan Zhang, Linjun Zhou, Renzhe Xu, Peng Cui, Zheyan Shen, and Haoxin Liu. Domain-irrelevant representation learning for unsupervised domain generalization. *arXiv preprint arXiv:2107.06219*, 2(3):4, 2021.

A Appendix

B Additional implementation details and results

B.1 Implementation details

Our work is implemented on an NVIDIA RTX 3080 GPU using PyTorch (Paszke et al., 2019). We use blank Resnet18 (He et al., 2016) as our feature extractor to align with the baseline (Menapace et al., 2020; Harary et al., 2022; Wang et al., 2022) The models in the first phase were trained using SGD with momentum 0.9 and weight decay $1e-4$. We use a batch size of 8 and train the model for 500 epochs. To train the clustering head, we use the same optimizer with batches of size 256 for 100 epochs for Office31 and Officehome datasets and 50 epochs for the PACS dataset. This difference is due to the small number of classes in the PACS dataset, which enables the model to converge much faster. To create style transfer augmentations, we use a pre-trained AdaIN model (Huang & Belongie, 2017). The most diversified head selection mechanism initiates at epoch 30 and is repeated every $n = 10$ epochs. For more information on the head selection mechanism, see the Multiple Clustering Heads section in the main text of our work. An important regularization for diversified training is label smoothing (Szegedy et al., 2016). Using pseudo-labels, we assume a high ratio of mislabeled samples; label smoothing helps prevent the model from predicting the training samples too confidently. The ablation study shows empirical evidence of the importance of label smoothing in our task.

B.2 Implementation of strong augmentations

In the pre-training phase 3.1, we perform style transfer or strong augmentations for each batch. When a batch is chosen to undergo strong augmentations, we use multiple augmentations which a chained together, creating the strong augmentation. Each augmentation component is chosen by a random probability. Those components include: random resized crop with a usage probability of $p = 0.8$, color jitter ($p = 0.8$), and parameters brightness=0.4, contrast=0.4, saturation=0.4, hue=0.1. Additional components are random grayscale ($p = 0.2$), horizontal flip ($p = 0.5$), and Gaussian blur ($p = 0.5$). Strong augmentation for the clustering head training 3.2 was done with the same strategies used in SCAN (Van Gansbeke et al., 2020): Cutout (DeVries & Taylor, 2017) and four randomly transformations from RandAugment (Cubuk et al., 2020).

B.3 Source of randomization between heads

Each head weight is initialized randomly using PyTorch(Paszke et al., 2019) default initialization. Since the classifier prediction determines the pseudo labels, each head will be trained using different pseudo labels; this variability will keep propagating as training proceeds.

B.4 Additional ablation studies

This section presents the results of an ablation study performed on three datasets. Tables 6,7,8 show results of our method without any smoothing, with label smoothing, and using prediction-based smoothing. In most cases, our proposed prediction-based smoothing is the best-performing method, illustrating its contribution to the overall method.

Table 6: Different label smoothing techniques ablation study results on the Officehome dataset (Venkateswara et al., 2017).

Method	$C, P, R \to A$	$A, P, R \to C$	$A, C, R \to P$	$A, C, P \to R$	Avg
No smoothing	20.6	25.2	27.1	27.3	25.0
Label smoothing	20.8	25.5	27.9	25.6	25.0
Prediction based smoothing	**20.8**	**26.2**	**27.7**	**27.2**	**25.5**

Table 7: Different label smoothing techniques ablation study results on the PACS dataset (Li et al., 2017).

Method	$C, P, S \to A$	$A, P, S \to C$	$A, C, S \to P$	$A, C, P \to S$	Avg
No smoothing	48.2	44.5	56.8	46.6	49.0
Label smoothing	46.3	44.4	**66.6**	**49.0**	51.6
Prediction based smoothing	**47.3**	**45.4**	**66.6**	48.0	**51.8**

Table 8: Different label smoothing techniques ablation study results on the Office31 dataset (Saenko et al., 2010).

Method	$D, W \to A$	$A, D \to W$	$A, W \to D$	Avg
No smoothing	24.0	50.0	47.4	40.4
Label smoothing	23.1	49.2	45.2	39.2
Prediction based smoothing	**24.1**	**50.1**	**47.7**	**40.6**

B.5 Sensitivity to hyperparameters

We perform a hyperparameter stability sensitivity study on different hyperparameters. We show that significant changes in hyperparameters do not lead to major changes in the performance of our proposed method. Specifically, we show a deviation of less than 6% in performance for all tested hyperparameter changes (see Table 9).

C Sample images

Figure 4 presents example images from the original domains and our BCD. Next, In Figure 5 we present sample images from datasets used in our paper.

Table 9: Hyperparameter stability results-p_{st} is the probability of doing style augmentation on the input data. p_{bcd} is the probability of transforming the input sample to the BCD, and $\#MDH$ is the number of cluster heads to keep during training.

Dataset	Variation	Hyper-parameter	Base value	Deviated value	Base Acc	Deviated Acc	Deviation
PACS	$A, P, S \rightarrow C$	p_{bcd}	0.2	0.3	44.7	44.1	1.34%
PACS	$A, P, S \rightarrow C$	p_{bcd}	0.2	0.4	44.7	46.1	3.13%
PACS	$A, P, S \rightarrow C$	p_{st}	0.3	0.2	44.7	45.0	0.67%
PACS	$A, P, S \rightarrow C$	p_{st}	0.3	0.4	44.7	45.6	2.01%
PACS	$A, P, S \rightarrow C$	MDHs	5	3	44.7	46.2	3.35%
PACS	$A, P, S \rightarrow C$	MDHs	5	7	44.7	46.6	4.25%
PACS	$A, C, S \rightarrow P$	p_{bcd}	0.2	0.3	66.6	64.8	2.70%
PACS	$A, C, S \rightarrow P$	p_{bcd}	0.2	0.4	66.6	66.2	0.60%
PACS	$A, C, S \rightarrow P$	p_{st}	0.3	0.2	66.6	62.8	5.71%
PACS	$A, C, S \rightarrow P$	p_{st}	0.3	0.4	66.6	63.6	4.50%
PACS	$A, C, S \rightarrow P$	MDHs	5	3	66.6	63.1	5.26%
PACS	$A, C, S \rightarrow P$	MDHs	5	7	66.6	65.3	1.95%
Officehome	$A, C, R \rightarrow P$	p_{bcd}	0.2	0.3	27.7	28.5	2.89%
Officehome	$A, C, R \rightarrow P$	p_{bcd}	0.2	0.4	27.7	26.8	3.25%
Officehome	$A, C, R \rightarrow P$	p_{st}	0.3	0.2	27.7	27.9	0.72%
Officehome	$A, C, R \rightarrow P$	p_{st}	0.3	0.4	27.7	27.8	0.36%
Officehome	$A, C, R \rightarrow P$	p_{st}	0.3	0.4	27.7	27.8	0.36%
Officehome	$A, C, R \rightarrow P$	MDHs	5	3	27.7	28.3	2.16%
Officehome	$A, C, R \rightarrow P$	MDHs	5	7	27.7	27.6	0.36%
Officehome	$A, C, P \rightarrow R$	p_{bcd}	0.2	0.3	27.2	27.4	0.74%
Officehome	$A, C, P \rightarrow R$	p_{bcd}	0.2	0.4	27.2	27.4	0.74%
Officehome	$A, C, P \rightarrow R$	p_{st}	0.3	0.2	27.2	27.0	0.74%
Officehome	$A, C, P \rightarrow R$	p_{st}	0.3	0.4	27.2	25.6	5.88%
Officehome	$A, C, P \rightarrow R$	MDHs	5	3	27.2	27.6	1.47%
Officehome	$A, C, P \rightarrow R$	MDHs	5	7	27.2	27.7	1.84%

Figure 4: Sample images from BCD domain for Officehome dataset (Venkateswara et al., 2017). The right and left columns show the original image and its BCD transform.

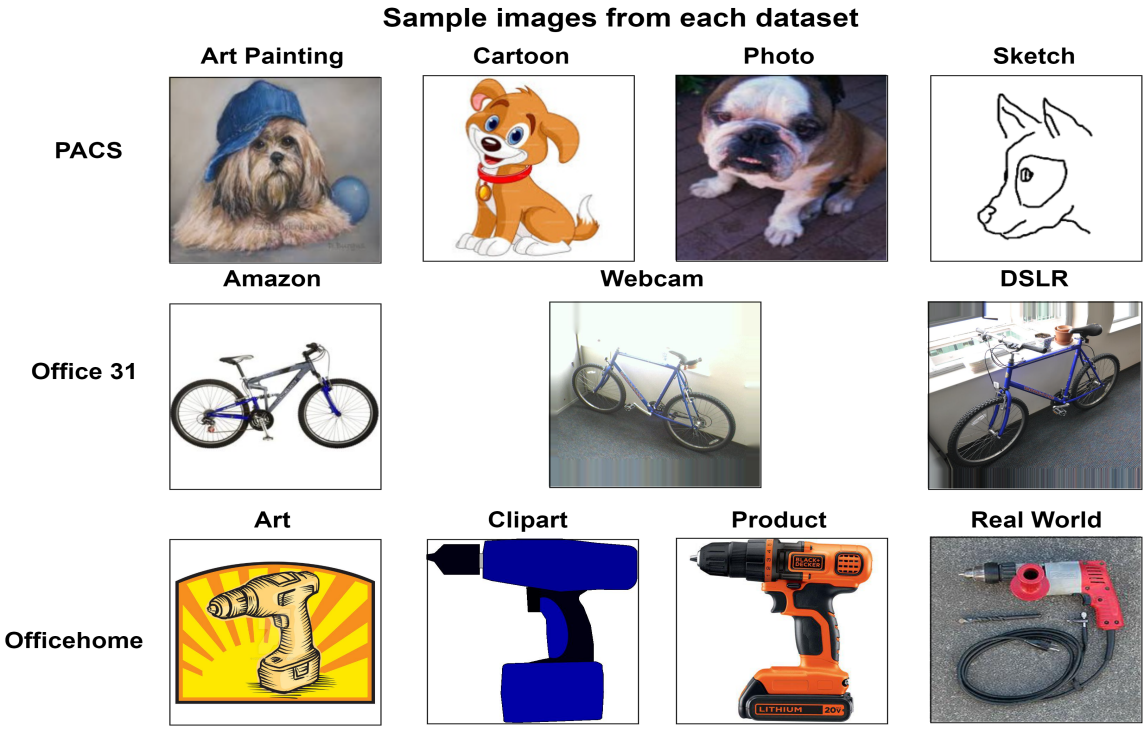

Figure 5: Sample images from the datasets used in the paper.